Monthly Notices
of the
ROYAL ASTRONOMICAL SOCIETY

Mon. Not. R. Astron. Soc. **425,** 2548–2556 (2012) doi:10.1111/j.1365-2966.2012.21724.x

CSS100603:112253−111037: a helium-rich dwarf nova with a 65 min orbital period

E. Breedt,[1⋆] B. T. Gänsicke,[1] T. R. Marsh,[1] D. Steeghs,[1] A. J. Drake[2] and C. M. Copperwheat[1]

[1]*Department of Physics, University of Warwick, Coventry*
[2]*California Institute of Technology, 1200 E. California Blvd, CA 91225, USA*

Accepted 2012 July 13. Received 2012 July 12; in original form 2012 June 20

ABSTRACT

We present time-resolved optical spectroscopy of the dwarf nova CSS100603:112253−111037. Its optical spectrum is rich in helium, with broad, double-peaked emission lines produced in an accretion disc. We measure a line flux ratio He I λ5876/Hα = 1.49 ± 0.04, a much higher ratio than is typically observed in dwarf novae. The orbital period, as derived from the radial velocity of the line wings, is 65.233 ± 0.015 min. In combination with the previously measured superhump period, this implies an extreme mass ratio of M_2/M_1 = 0.017 ± 0.004. The Hα and He I λ 6678 emission lines additionally have a narrow central spike, as is often seen in the spectra of AM CVn-type stars. Comparing their properties with cataclysmic variables (CVs), AM CVn systems and hydrogen binaries below the CV period minimum, we argue that CSS100603:112253−111037 is the first compelling example of an AM CVn system forming via the evolved CV channel.

With the addition of this system, evolved CVs now account for 7 per cent of all known semidetached white dwarf binaries with $P_{\rm orb} < 76$ min. Two recently discovered binaries may further increase this figure. Although the selection bias of this sample is not yet well defined, these systems support the evolved CV model as a possible formation channel for ultracompact accreting binaries. The orbital periods of the three ultracompact hydrogen accreting binaries overlap with those of the long-period AM CVn stars, but there are currently no known systems in the period range of 67–76 min.

Key words: binaries: close – stars: dwarf novae – stars: individual: CSS100603:112253−111037 – novae, cataclysmic variables.

1 INTRODUCTION

Cataclysmic variable stars (CVs) typically consist of a white dwarf and a near main-sequence, late-type star in a close binary orbit, with the defining characteristic that mass is transferred from the companion to the white dwarf through Roche lobe overflow. (See Warner 1995 for a detailed review of CVs.)

A subset of CVs shows quasi-periodic brightenings of several magnitudes, known as dwarf nova outbursts. These outbursts are thought to be the result of a thermal instability in the accretion disc which forms around the white dwarf (Osaki 1989), and detection through outbursts remains an important method through which new CVs are discovered (e.g. Gänsicke 2005; Drake et al. 2009). Some dwarf novae also show superoutbursts, which last longer than the normal outbursts and are generally brighter. During superoutbursts, the accretion disc becomes axially asymmetric due to tidal interaction with the donor star. The resulting tidal stresses and stream interaction with the outer disc are observed as a photometric modulation in the light curve, known as superhumps. The superhump period is closely related to the mass ratio of the system and is a good proxy for the orbital period, being typically only a few per cent longer than the orbital period (e.g. Patterson et al. 2005; Gänsicke et al. 2009; Kato et al. 2009; Wood et al. 2011).

Through the process of angular momentum loss, CVs evolve from long to short orbital periods, to a minimum period $P_{\rm min}^{\rm CV}$. The period minimum occurs at the point where the donor star is driven so far out of thermal equilibrium by the mass-loss that it can no longer shrink rapidly enough to attain thermal equilibrium, i.e. the thermal time-scale of the donor star is longer than the mass-loss time-scale. Further, mass-loss therefore requires the orbit to expand to accommodate the donor, so the system evolves back to longer periods. (See e.g. Rappaport, Joss & Webbink 1982; Kolb & Baraffe 1999.) If the donor is partially degenerate, further mass-loss will cause its

⋆E-mail: e.breedt@warwick.ac.uk

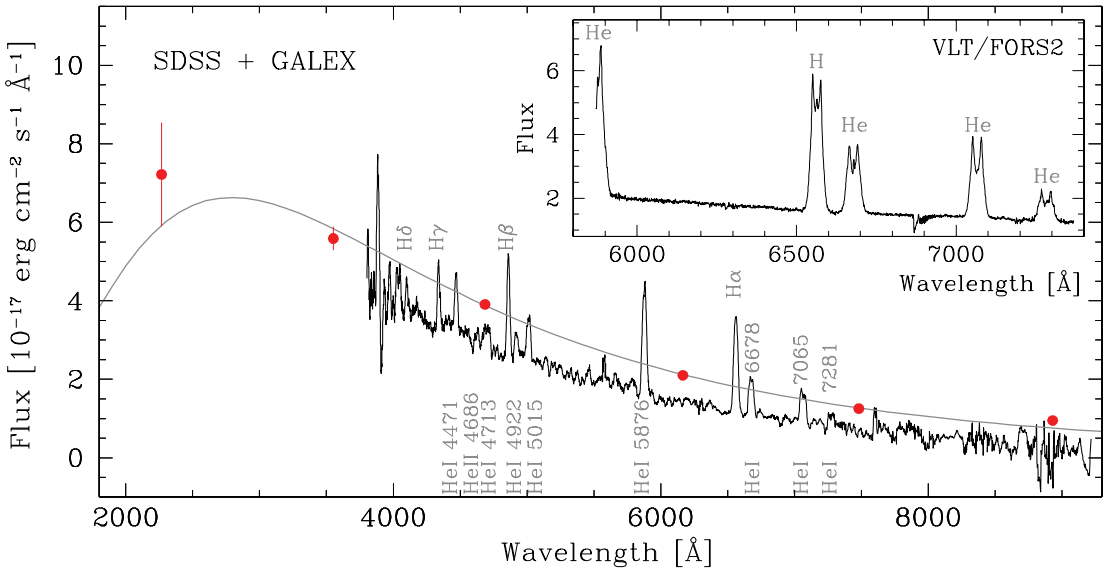

Figure 1. Main panel: optical spectrum of CSS1122−1110 from the SDSS, with the strongest emission lines labelled. The SDSS spectrum was smoothed by a 15-point box car for display purposes. The grey line overplotted on the spectrum is a blackbody of $T = 10\,400$ K, fitted to the SDSS and *GALEX* fluxes (red dots). The offset between the photometric and spectroscopic measurements is likely due to the variability of the source. The spectrum and the photometric measurements were corrected for Galactic extinction. Inset: average spectrum from our VLT/FORS2 observations.

radius to grow, accelerating the process. The period minimum is observed to be $P_{\rm min}^{\rm CV} \sim 80$ min in hydrogen-rich systems (Gänsicke et al. 2009).

By definition, the donor stars in CVs fill their Roche lobes, which for a given orbital period define the density of the donor star. For orbital periods much shorter than $P_{\rm min}^{\rm CV}$, the density of a Roche lobe filling star will be higher than those for typical main-sequence stars, which implies that the donor has to be evolved or degenerate. At present, only 42 ultracompact accreting binaries with $P_{\rm orb} < 76$ min are known (Section 4). Almost all of these belong to the small class known as AM CVn stars (see Solheim 2010 for a recent review). Their donor stars are generally deficient of hydrogen, allowing them to have very short orbital periods, observed to be in the range of 5–65 min. The white dwarf primary in AM CVn systems accretes either from another less massive, white dwarf (Paczyński 1967; Faulkner, Flannery & Warner 1972), from a low-mass semidegenerate helium star (Savonije, de Kool & van den Heuvel 1986; Iben & Tutukov 1987), or from an evolved main-sequence star which has lost its hydrogen envelope (Podsiadlowski, Han & Rappaport 2003). Only in HM Cnc, the shortest period AM CVn system, has hydrogen been detected in the optical spectrum (Roelofs et al. 2010). There are three different AM CVn formation channels, characterized by the three types of donor stars seen in these systems. Their relative importance has been a long-standing question. Population synthesis models suggest that the evolved CV channel is unimportant compared to the white dwarf and helium star channels, mainly because of the long evolutionary time-scales required (e.g. Nelemans, Yungelson & Portegies Zwart 2004; Nelemans et al. 2010; Yungelson et al., in preparation). These calculations are however sensitive to the specific form of the magnetic braking model used (van der Sluys, Verbunt & Pols 2005a,b), and Podsiadlowski et al. (2003) argue that a noticeable fraction of AM CVn stars could form from CVs with evolved donor stars.

In this paper, we present optical spectroscopy of CSS100603:112253−111037 (hereafter CSS1122−1110), a helium-dominated binary which is evolving along the CV track to become an AM CVn system. It was discovered in an outburst on 2010 June 3 by the Catalina Real-Time Transient Survey (CRTS; Drake et al. 2009), at a magnitude of 14.3. It was followed up photometrically by VSNET[1] (Variable Star Network) observers (Kato 2010; Maehara 2010a,b), who reported a superhump period of $P_{\rm sh} = 65.434 \pm 0.040$ min (Kato et al. 2010). An optical spectrum of this system is available from the Sloan Digital Sky Survey (SDSS; Abazajian et al. 2009), shown in Fig. 1. It reveals a blue continuum dominated by He I emission, along with obvious hydrogen Balmer emission lines. Subsequently, CSS1122−1110 was also included in the SDSS CV catalogue of Szkody et al. (2011),[2] who also noted the unusual helium-to-hydrogen line ratios in this binary.

2 OBSERVATIONS

2.1 Optical spectroscopy

We carried out time-resolved spectroscopy of CSS1122−1110 over three nights in 2011 March, using the FORS2 spectrograph at the European Southern Observatory (ESO) Very Large Telescope (VLT) at Paranal, Chile. Observing conditions were very good, with subarcsecond seeing throughout. We used the GRIS 1200R+93 grism with a 1 arcsec slit and 2 × 2 binning of the 2k × 4k MIT CCD. The resulting spectra cover the spectral range 5872–7370 Å with an average dispersion of 0.73 Å per binned pixel and a full width at half-maximum (FWHM) resolution of 1.7 Å.

We obtained 52 spectra in total over the three nights, covering approximately two binary orbits on the first night, two on the second night and one orbit on the last night. All spectra were taken using an exposure time of 420 s, except for one exposure on the second night which was aborted after 177 s due to a temporary guiding error of the telescope. The spectra were reduced using the STARLINK[3]

[1] http://www.kusastro.kyoto-u.ac.jp/vsnet/
[2] Referred to as SDSS J112253.3−111037.6.
[3] http://starlink.jach.hawaii.edu/starlink

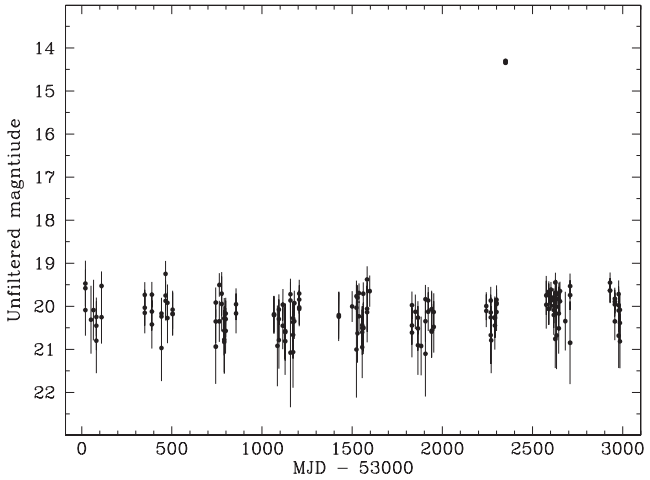

Figure 2. CSS light curve spanning eight years of observations. The average quiescent magnitude is 20.2 ± 0.5 and the outburst reached a magnitude of 14.3.

packages KAPPA and FIGARO, and optimally extracted using PAMELA[4] (Marsh 1989).

The wavelength calibration is based on helium–argon–neon arc lamp exposures which were taken during the day. We identified 25 reliable arclines over the spectral range and fitted them with a fifth-order polynomial. The root mean square of the fit residuals was 0.012 Å. In order to account for a small amount of flexure of the instrument, we shifted the spectra so that the strong night-sky emission line at 6300.304 Å appears at its known wavelength. The typical shifts required were 0.1–0.2 pixels.

The instrumental response and flux calibration were calculated from a spectroscopic standard star observed at the start of each night as part of the ESO calibration programme. The spectra from the first and third nights were calibrated using HD 49798 and the second night's spectra were calibrated against Hiltner 600. The spectra are not corrected for telluric absorption or slit losses, so the flux calibration is not absolute. However, the continuum slope and the relative calibration over the three nights are reliable.

2.2 Photometry

The Catalina Sky Survey (CSS) has visited the field containing CSS1122−1110 256 times since the start of the survey. Our target was undetected on 82 of these images, and we rejected a further six for which the measured photometric error exceeded 8 per cent (compared to the mean error of 2.3 per cent). This left 168 reliable photometric measurements. The median time between CRTS visits is 19 d, with typically two to four observations per visit, taken over 30–40 min. The light curve, spanning 8.1 yr, is shown in Fig. 2. Only one outburst was seen during this time. We measure an average unfiltered quiescent magnitude of 20.2 ± 0.5, in good agreement with the SDSS magnitudes.

We also carried out differential photometry on our VLT/FORS2 acquisition images, using IRAF.[5] The acquisition was done using the R_SPECIAL+76 filter, a broad-band filter centred on 6550 Å with an FWHM of 1650 Å. It therefore includes all four lines in our spectrum. The photometry showed that the object brightened by 0.15 ± 0.02 mag over the three nights of observations.

[4] PAMELA is included in the STARLINK distribution 'Hawaiki' and later releases.
[5] IRAF is distributed by the National Optical Astronomy Observatory, which is operated by the Association of Universities for Research in Astronomy under cooperative agreement with the National Science Foundation.

Table 1. Spectral energy distribution.

Band	$\lambda_{\rm eff}$ (Å)	Magnitude	Error
GALEX near-UV	2267	21.65	0.22
SDSS-*u*	3551	20.71	0.06
SDSS-*g*	4686	20.44	0.02
SDSS-*r*	6165	20.46	0.03
SDSS-*i*	7481	20.57	0.04
SDSS-*z*	8931	20.46	0.12

3 ANALYSIS AND RESULTS

3.1 Spectral energy distribution

The ultraviolet (UV) and optical magnitudes of CSS1122−1110, as given by the *GALEX* (Galaxy Evolution Explorer; Martin et al. 2005) Data Release 6 and SDSS Data Release 8 (Aihara et al. 2011), are shown in Table 1. The system is undetected in the *GALEX* far-UV band. Correcting for Galactic extinction towards the source, $E(B-V) = 0.048$ (Schlegel, Finkbeiner & Davis 1998), the photometric measurements are well described by a $T = 10\,400 \pm 300$ K blackbody spectrum, shown as a grey line in Fig. 1. The flux difference between the photometric and spectroscopic SDSS measurements is due to the variability of the source. A lower limit on the distance to the system can be set by assuming that the continuum emission originates from the white dwarf only, with no disc contribution. Assuming a typical white dwarf radius of 0.01 $R_\odot$, this gives $d \geq 345$ pc.

3.2 Emission line profiles

We show the average line profiles of the four emission lines visible in our FORS2 spectra in Fig. 3. Unfortunately, much of the He I λ 5876 emission line is lost from the blue end of the CCD, so this line is not usable for analysis. The lines are broad and display a classic double-peaked profile, revealing the presence of an accretion disc. The Hα and He I λ6678 lines additionally have a narrow emission component at the line centre. The He I λλ 7065 and 7281 lines show no such component. Such a 'central spike' is never seen in the spectra of CVs, but many AM CVn systems display this feature,[6] e.g. GP Com (Smak 1975; Marsh 1999), V396 Hya (CE315; Ruiz et al. 2001) and SDSS J124058.03−015919.2 (Roelofs et al. 2005). In these systems, the central spikes display radial velocity variations consistent with emission from near the white dwarf (Morales-Rueda et al. 2003). A similar narrow emission line originating from near the white dwarf is seen in some detached post-common-envelope binaries (e.g. LTT 560; Tappert et al. 2011b, but see also Tappert et al. 2011a and fig. 8 of Gänsicke et al. 2004). The white dwarf in LTT 560 is accreting from the wind of its companion, and the

[6] For completeness, we note that the Hα emission line in the CV SDSS J003941.06+005427.5 is triple-peaked (Southworth et al. 2010), but unlike the central spike observed in AM CVn stars, it has a large radial velocity amplitude (202 km s^{-1}) which does not match the expected velocities of the white dwarf, the secondary star or the accretion disc bright spot. Southworth et al. (2010) suggest that it may originate from a coronal loop on a magnetically active secondary star, similar to those which have been observed in outburst spectra of IP Peg and SS Cyg (Steeghs et al. 1996).

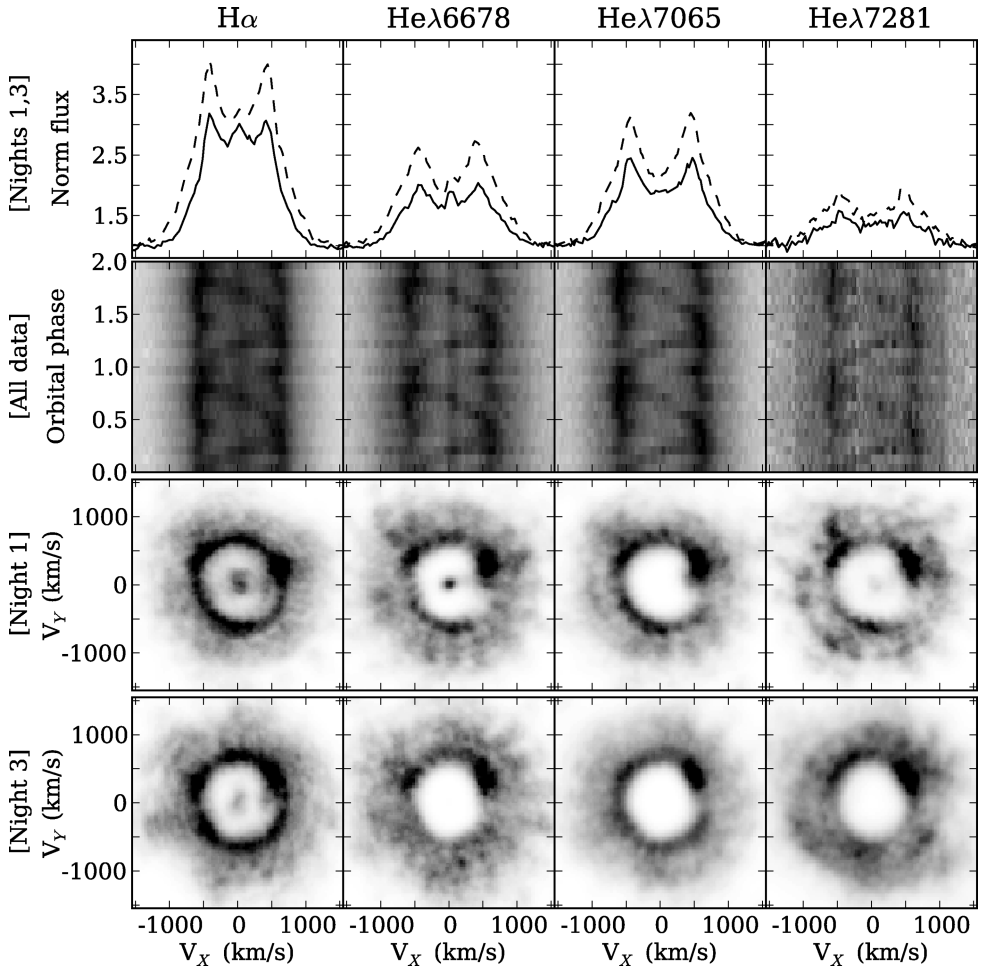

Figure 3. Top row: average, continuum normalized emission line profiles from the first (solid line) and third (dashed line) nights of observations on VLT/FORS2. The double-peaked profile is characteristic of Doppler motion in an accretion disc. On the first and second night, the Hα and He I λ 6678 lines additionally show a narrow component at the centre of the line. The lines also get broader as they get brighter, indicating that the emission originates from a higher velocity region. This is true even if the lines are normalized to the line peaks. The vertical axis is the same for all four line profiles for ease of comparison. Second row: trailed spectra from all three nights, normalized to the continuum and folded on the orbital period. Two orbital cycles are shown for clarity. The panels were scaled individually to the minimum and maximum flux in each panel. Third row: the Doppler maps calculated from the first night's spectra. The central spike of the emission line maps to a bright spot at the origin of the map, consistent with the expected velocity position of the white dwarf. Bottom row: the Doppler maps calculated from the third night's spectra. The white dwarf emission component has disappeared, as it is dominated by the disc emission. The Doppler maps are subject to an unknown rotation compared to the coordinate system such maps are usually displayed in (see the text), as the zero phase of the white dwarf is not known. We used $\mathrm{BJD_0} = 245\,5646.6655$ as in Fig. 4.

emission is thought to originate in a chromosphere or corona around the white dwarf which forms as a result of the accretion activity.

The central spike in CSS1122−1110 is too weak and its variations are too small to reliably measure the radial velocity amplitude with a moving Gaussian model. The trailed spectra in Fig. 3 show that it is stationary at the line centre to within 1 pixel (33 km s^{-1}). Future observations will greatly benefit from using a shorter exposure time per spectrum to reduce the amount of orbital smearing of the spike, which will allow us to track the small amplitude variations with greater precision.

We observed an increase in line and continuum flux over the three nights of observations. In order to quantify the variability, we shifted the emission lines to their zero velocity position and calculated the average of each night's spectra. The equivalent widths, as measured from these average spectra, are shown in Table 2. The equivalent widths increase by a factor of $\gtrsim$1.5 from the first to the third night. The line flux increased by a factor of 1.6 during the same time, and the continuum, as measured from a line-free part of the spectrum (50 Å centred on 6100 Å), brightened by a factor of 1.2. The brightness increase is consistent with the magnitude change measured from the acquisition images (Section 2.2). No periodic signal is detected in the continuum variations. We note that, as the system became brighter, the central spike became harder to detect and the lines became slightly broader. The central spike is completely absent from the He I λ 6678 line on the third night

Table 2. Line equivalent width variation over the three nights of observations.

	Equivalent width (Å)		
Line	n1	n2	n3
Hα	76	95	113
He I λ 6678	40	54	69
He I λ 7065	49	65	78
He I λ 7281	20	25	35

(see Fig. 3), and barely detected in Hα. We interpret this behaviour as variability originating in the accretion disc, outshining the coronal or chromospheric emission from the white dwarf as it brightens, causing the central spike to disappear from the spectrum.

3.3 Orbital period

To measure the radial velocity variation, we used the double Gaussian technique of Schneider & Young (1980) and Shafter (1983), as implemented in MOLLY.[7] This measurement is sensitive to the high-velocity line wings which originate in the inner disc and is often used as an indication of the radial velocity of the white dwarf (e.g. Thorstensen 2000).

We used two Gaussian functions of FWHM = 400 km s^{-1} to account for the broad emission lines, and varied the separation between the peaks from 800 to 3000 km s^{-1}. For each resulting radial velocity curve, we calculated the Lomb–Scargle periodogram (Lomb 1976; Scargle 1982) and then folded the radial velocities on the strongest period. The folded radial velocity curve was then fitted with a circular orbit of the form

$$V(t) = K \sin[2\pi(t - \mathrm{BJD}_0)/P_{\mathrm{orb}}] + \gamma\,, \quad (1)$$

where the reference time BJD_0 is defined by the blue to red crossing of the measured velocities.

A diagnostic diagram analysis (Shafter, Szkody & Thorstensen 1986) showed that σ/K is minimum for a separation of 1200 km s^{-1}, where σ is the scatter around the fit. This separation also gives a consistent orbital period and reference time from all four emission lines. We show the Lomb–Scargle periodogram calculated from the He I λ 7065 radial velocities in Fig. 4. The strongest signal occurs at a frequency of 22.075 cycles d^{-1}, corresponding to a period of 65.233 min. The nearest competing peaks are the $\pm$1 d aliases at 21.058 and 23.064 cycles d^{-1}. We carried out 10 000 bootstrap selections of the radial velocity curve, calculated the periodogram of each of these randomly selected subsets and recorded the strongest peak. 98.95 per cent of the radial velocity subsets resulted in 22.074 cycles d^{-1} as the strongest signal. 0.6 per cent of the subsets found the 21.058 cycles d^{-1} alias marginally stronger, and only 0.45 per cent preferred the alias at 23.064 cycles d^{-1}. Thus, we are confident that the strongest signal is the correct identification of the spectroscopic period of this CV. The He I λ 7065 radial velocity curve, folded on this period, is shown in the middle panel of Fig. 4. The parameters of the best fit of equation (1), as derived from the three strongest lines, are listed in Table 3.

The bottom panel of Fig. 4 shows the Hα radial velocities folded on the same period. The amplitude of the variations is much smaller than those derived for the helium lines and the curve is highly non-sinusoidal. Its sawtooth shape suggests that the emission region is non-circular. A non-circular emission region is also supported by the shape of the Hα Doppler map (Section 3.5) in Fig. 3. Even though we derive a consistent period from the four available emission lines, the amplitudes of the variation differ by several tens of km s^{-1} and in all cases are much larger than expected for the white dwarf in such a compact binary. This is a clear indication that the phase-dependent modulation of the line wings is not purely a result of the radial velocity of the white dwarf. The high-velocity wings of the emission lines contain flux from other bright regions of the disc, e.g., the bright spot, and cannot be used to track the motion of the white dwarf in this case.

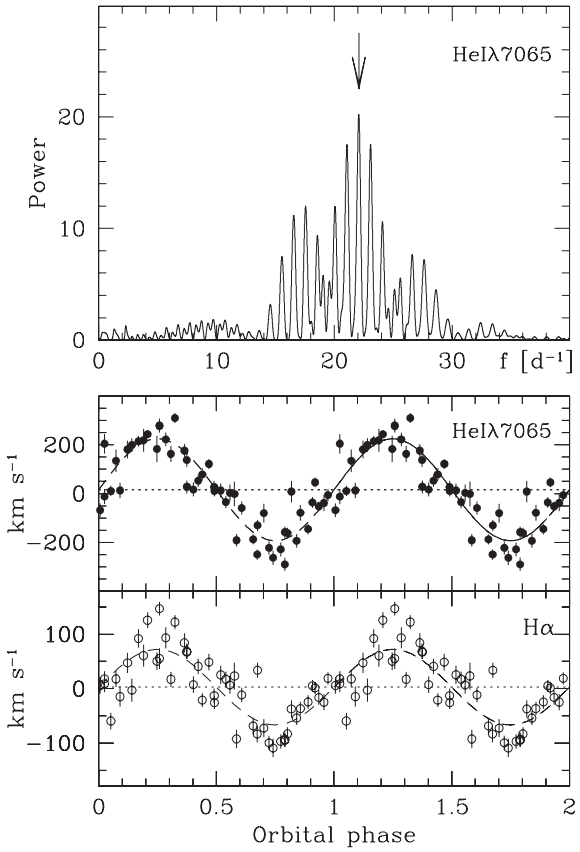

Figure 4. Top panel: Lomb–Scargle periodogram calculated from the He I λ 7065 radial velocities of CSS1122−1110. The adopted orbital frequency is indicated by an arrow. Middle panel: the measured He I λ 7065 radial velocities folded on a period of 65.233 min. The dashed line is the best-fitting sinusoid to the radial velocities and its parameters are shown in Table 3. Two phases are plotted for clarity. Bottom panel: the Hα radial velocities, folded on the same period. Note the smaller amplitude compared to the He radial velocity variation.

In an effort to isolate the bright-spot emission to measure its velocity amplitude more accurately, we subtract from each spectrum the average spectrum from that night. This removes the constant flux, and leaves only the variable part of the emission. The signal-to-noise ratio is not high enough to fit these residuals in the individual spectra with a moving Gaussian to measure the period, but when folded on the period determined above, the disc bright-spot emission clearly shows up in the Doppler maps and as an *S*-wave in the trailed spectra. The *S*-wave is also clearly visible in the continuum normalized spectra shown in the second row of Fig. 3. Incidentally, folding the residuals on either of the 1 d aliases smears the emission out completely, so that no structure is visible in the trailed spectra. This is a further confirmation that we have selected the correct alias as the orbital period. Measuring the bright-spot velocity from the phase-binned spectra yields a semi-amplitude of 550 $\pm$ 27 km s^{-1} for the He I λ7065 line, 575 $\pm$ 28 km s^{-1} for the He I λ6678 line and 506 $\pm$ 16 km s^{-1} for Hα (Table 3).

3.4 Binary mass ratio

Superhumps are characteristic of dwarf novae in superoutburst (Whitehurst 1988; Hirose & Osaki 1990). A resonant interaction

[7] MOLLY was written by Marsh and is available at http://www.warwick.ac.uk/go/trmarsh/software/

Table 3. Orbital properties as derived from each of the strongest emission lines.

	Hα	He I λ 6678	He I λ 7065
$P_{\rm orb}$(d)	0.045 29(2)	0.045 32(1)	0.045 30(1)
BJD$_0$	245 5646.6660(3)	245 5646.6663(2)	245 5646.6655(2)
K (km s^{-1})	69.4 $\pm$ 2.9	285.8 $\pm$ 5.8	208.4 $\pm$ 5.1
γ (km s^{-1})	2.8 $\pm$ 2.0	32.6 $\pm$ 4.7	16.1 $\pm$ 3.6
Bright-spot velocity (km s^{-1})	505.8 $\pm$ 15.7	575.0 $\pm$ 28.3	549.9 $\pm$ 26.5

between the outer accretion disc and the donor star causes periodic flexing of the disc, which compresses the disc on the side opposite to the donor star and increases the viscous dissipation in this region. The observed brightness modulation is known as superhumps. During the later stages of the outburst, variable dissipation from the bright spot also contributes to the superhump signal, as it sweeps around the edge of the asymmetric disc. See Wood et al. (2011) for a detailed discussion of the origin of superhumps. The dynamical nature of this phenomenon means that there is good reason to expect the superhump period, $P_{\rm sh}$, to be related to the mass ratio q of the binary. Specifically, it is the superhump excess, $\epsilon = (P_{\rm sh} - P_{\rm orb})/P_{\rm orb}$, which is found to correlate well with q (e.g. Patterson et al. 2005). This empirical relation is derived from eclipsing dwarf novae, for which the mass ratio and superhump excess can be measured independently.

There are three similar formulations of the $\epsilon - q$ relation which are commonly used, but unfortunately the low-ϵ end of the relation is poorly constrained by observations. Patterson et al. (2005) find $\epsilon = 0.18\,q + 0.29\,q^2$ and Kato et al. (2009) give an updated version as $\epsilon = 0.16\,q + 0.25\,q^2$. Both of these formulations assume that $\epsilon = 0$ when $q = 0$. This is a reasonable assumption, since for a negligible secondary mass, we would expect the tidal interaction with the disc to become negligible as well. Observations of the only known eclipsing AM CVn system, SDSS J0926+3624 (Copperwheat et al. 2011), agree best with the Patterson et al. (2005) relation, so we favour that version in the calculations below. For completeness, we also note the third formulation of the $\epsilon - q$ relationship, as given by Knigge (2006), $q = (0.114 \pm 0.005) + (3.97 \pm 0.41) \times (\epsilon - 0.025)$. Here, the assumption $\epsilon = 0 = q$ is not made, so the value of q is probably overestimated for this binary.

Using our spectroscopically determined period and the superhump period measured by Kato et al. (2010), we find a small superhump excess in CSS1122−1110, $\epsilon = 0.0031 \pm 0.0007$. This implies an extreme mass ratio, $q = 0.017 \pm 0.004$. For the average white dwarf mass found in CVs, $M_1 = (0.83 \pm 0.23)\,{\rm M}_\odot$ (Zorotovic, Schreiber & Gänsicke 2011), this implies a very low mass donor, $M_2 = (0.014 \pm 0.005)\,{\rm M}_\odot$.

3.5 Doppler tomography

The second row of Fig. 3 shows the trailed spectra, centred on each of the emission lines covered by our FORS2 spectra. The spectra from all three nights are included in these trails, each normalized to the continuum and then folded on the orbital period. The central spike is visible as a faint line at the line centres of Hα and He I λ 6678, and an *S*-wave is seen in all four trails.

We computed corresponding Doppler tomograms (Marsh & Horne 1988) for each of the emission lines, for each night separately, as well as phase-binned together over the three nights. The increase in the line width as the system gets brighter blurs the map when the spectra from all three nights are included in a single map, so instead we show the maps calculated from the first and the third nights' spectra separately, in the third and fourth row of panels in Fig. 3. The maps from the second night's spectra are near identical to those from the first night. All maps were calculated using BJD$_0$ = 245 5646.6655 as a phase zero reference time, as derived from the radial velocities of the He I λ 7065 line wings in Section 3.3. The resulting maps are clearly rotated with respect to the standard orientation usually used in these displays, which has the white dwarf and donor star aligned along the vertical $V_X = 0$ axis (Marsh & Horne 1988). In that orientation, the disc bright spot appears in the upper-left quadrant of the map. This rotation seen here is a result of the unknown phase shift between our choice of BJD$_0$ and true zero phase of the white dwarf. All the maps show a similar structure, with a bright ring corresponding to emission from the accretion disc, a bright spot on the disc rim (equivalent to the *S*-wave in the trailed spectra) and a small spot at the origin of the map, which corresponds to the central spike seen in the average Hα and He I λ 6678 line profiles. We measured the velocity position of the central spike by fitting it with a two-dimensional Gaussian function. Its velocity is consistent with zero, so we are not able to use it to determine the zero phase orientation of the map. We have observed more than one binary orbit per night, so we have also calculated Doppler maps for each orbit individually. From the position of the central spot in these, and the combined maps, we can constrain the radial velocity of the white dwarf to $K_1 < 16$ km s^{-1}. On the third night of our observations, when the system was at its brightest, the emission was dominated by the accretion disc. As a result, the central spot disappeared completely from the He I λ 6678 map, and only some weak emission remained at this position in the Hα map.

As an illustration, we overplot the He I λ 6678 map with the Roche lobe parameters of a $q = 0.017$ binary in Fig. 5. The assumed velocity positions of the white dwarf, donor star and velocity streams are also shown. We stress that, since the zero phase of the white dwarf is not known, we have the freedom to rotate the map about its origin, so this combination of parameters is not a unique description of this Doppler map. It only serves as an illustration of the extreme mass ratio $q = 0.017$, as determined from the $\epsilon - q$ relation in the previous section.

4 DISCUSSION

Three channels are thought to contribute to the formation of AM CVn stars. (a) A double-degenerate channel, where a white dwarf accretes from another, helium-rich white dwarf (Paczyński 1967; Faulkner et al. 1972). This ultracompact configuration requires a second common envelope phase during the evolution to shorten the period to the observed values, in addition to angular momentum loss by gravitational radiation. Potential direct progenitors for this type of binary are the detached double white dwarf systems, in particular those with extremely low mass white dwarf companions (Brown et al. 2011, 2012). (b) An alternative outcome of a double common envelope evolution is that the donor star is not fully degenerate when it leaves the common envelope (Savonije

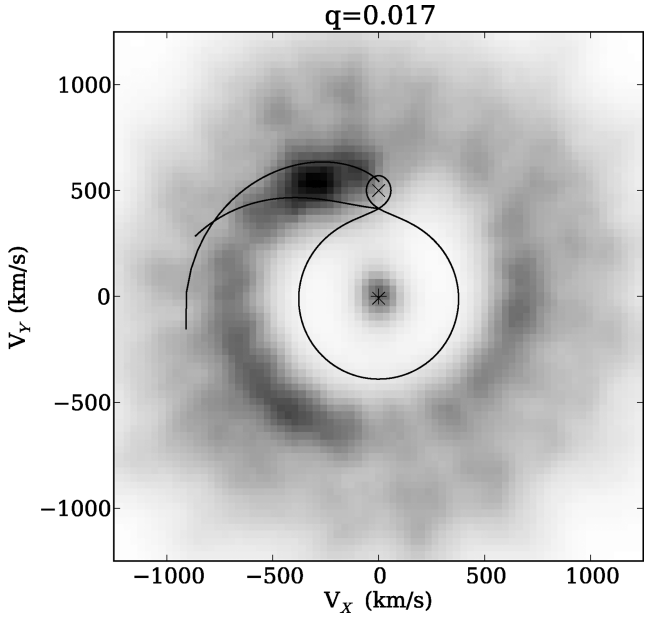

Figure 5. He I λ 6678 Doppler map overplotted with the Roche lobes of a $q = 0.017$ binary. The assumed velocities of the white dwarf and donor star are labelled with the × symbol and the centre of mass velocity at (0, 0) with a + symbol. The map was rotated by applying a −0.25 phase shift compared to the maps shown in Fig. 3.

et al. 1986; Iben & Tutukov 1987). The system starts mass transfer with the donor in the helium burning stage and the donor becomes increasingly degenerate as it evolves towards the period minimum of ∼10 min. (c) If the initial separation is too large for a second common envelope to form, the system may evolve as a CV. An ultracompact binary may form if the initial mass ratio is such that the donor star undergoes significant nuclear evolution before the onset of mass transfer (Podsiadlowski et al. 2003). The density of the evolved donor allows the system to reach a much shorter orbital period than is possible for the hydrogen CVs, with the exact value depending on the level of hydrogen depletion in the donor when the mass transfer starts (e.g. Sienkiewicz 1984). The donor stars in these systems will have some hydrogen left in their envelopes as they evolve towards their period minima, but will become increasingly helium rich during the evolution. This is the only formation channel in which the donor is predicted to have residual hydrogen in its envelope, so the detection of hydrogen in the spectrum of an AM CVn binary conclusively identifies it as having evolved along this track (Podsiadlowski et al. 2003; Nelemans et al. 2010).

The evolved CV formation channel is often dismissed as improbable or unimportant compared to the other channels, since it would require an evolutionary time-scale comparable to, or even exceeding, the Hubble time to reach periods as short as those observed in AM CVn systems, if angular momentum loss is driven by magnetic braking and gravitational radiation (Nelemans et al. 2010; Yungelson et al., in preparation). From population synthesis models, Nelemans et al. (2004) estimate that less than 2 per cent of AM CVn binaries can form this way. However, if the initial mass ratio is $q \gtrsim 1$, the binary will undergo a period of thermal time-scale mass transfer (TTMT) until the mass ratio decreases to $q \lesssim 5/6$, allowing stable mass transfer (Tutukov et al. 1985; Pylyser & Savonije 1989; Schenker et al. 2002). The rapid mass-loss strips the donor from its hydrogen envelope, exposing the partially evolved core. When the system resumes normal mass transfer and angular momentum loss, it will appear essentially as a normal CV, except that the donor will be evolved compared to other CVs at the same orbital period. Those systems in which most of the hydrogen is lost during the period of TTMT will be able to evolve to periods well below $P_{\rm min}^{\rm CV}$. Since the rapid mass transfer also removes angular momentum at a high rate, it is possible for these systems to evolve to ultrashort periods within a Hubble time. The fraction of CVs with evolved secondaries is expected to be high. Podsiadlowski et al. (2003) put this figure at 10 per cent, and Schenker et al. (2002) suggest a fraction as high as a third.

Observations of V485 Cen (59 min; Augusteijn, van Kerkwijk & van Paradijs 1993; Augusteijn et al. 1996) and EI Psc (64 min; Thorstensen et al. 2002) support the idea that binaries which have undergone TTMT can evolve to an ultracompact configuration. The optical spectrum of EI Psc shows a donor star with spectral type K4±2 (Thorstensen et al. 2002), which is anomalously hot for a main-sequence star at such a short orbital period. Its UV spectrum also reveals a low carbon to nitrogen abundance (Gänsicke et al. 2003), indicating that the accreted material is CNO processed, so the white dwarf is accreting from the exposed, evolved core. Apart from V485 Cen, EI Psc and CSS1122−1110, there are two more short-period binaries which are candidates for AM CVn progenitors of the 'evolved CV' channel: CSS090331:102843−081927 (52 min; Woudt et al. 2012, hereafter CSS1028−0819) and CSS111019:233313−155744 (62 min, Woudt & Warner 2011, hereafter CSS2333−1557). At the moment, little is known about either of these systems. CSS1028−0819 was discovered in outburst by the CRTS and subsequent outburst photometry revealed a period excess of $\epsilon = 0.0530$ (Woudt et al. 2012). VSNET observers (Kato & Kinugasa 2009) reported the outburst spectrum to show both hydrogen and helium lines. No spectroscopic observations of CSS2333−1557 are available yet to determine whether it is an AM CVn system, a hydrogen accreting binary or a halo CV.[8]

There are only 42 semidetached binaries known with periods below $P_{\rm min}^{\rm CV}$: 36 AM CVn systems, one low-metallicity halo CV, three ultracompact hydrogen accreting binaries and two binaries discovered as a result of outburst activity, but still of unknown nature. The three confirmed ultracompact hydrogen accretors (CSS1122−1110, V485 Cen and EI Psc) therefore account for 7 per cent of this total. If CSS1028−0819 and CSS2333−1557 are confirmed as hydrogen accreting systems as well, this figure will rise to 12 per cent. Although these figures do not take selection effects into account, such a high fraction of possible progenitors suggests that the evolved CV channel is non-negligible when considering AM CVn formation. A statistically complete sample of ultracompact accreting binaries is not yet available.

We show the cumulative period distribution of all accreting white dwarf binaries with known orbital periods in Fig. 6. In the period range 59–66 min, both long-period AM CVn stars and short-period hydrogen accreting systems are found, but currently there are no known systems with periods between 67 and 76 min. This is surprising, because if the critical parameter which determines

[8] One more short-period hydrogen accreting binary is known, SDSS J150722.30+523039.8 (67 min; Littlefair et al. 2007). It is excluded from the discussion, as it has been shown to be a CV in the Galactic halo, with a low-mass Population II donor star (Uthas et al. 2011). Its short period stems from the lower atmospheric opacity of such a low-metallicity star, which means that it has a smaller radius and fills its Roche lobe at shorter orbital periods.

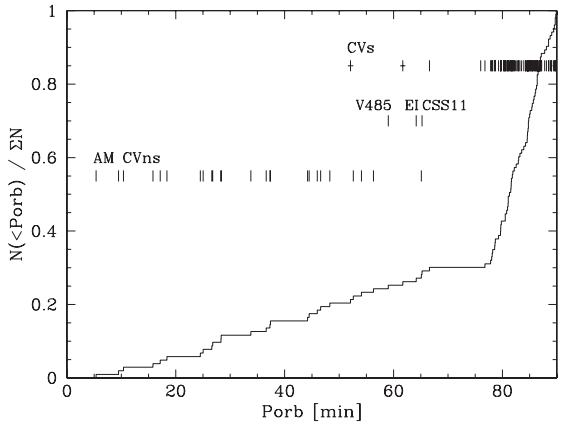

Figure 6. Cumulative period distribution of all AM CVn stars, CVs with $P_{\rm orb} < 90$ min and short-period hydrogen accreting binaries with known orbital periods. AM CVn stars span the period range 5–65 min, CVs the range 76 min and longer and the ultracompact hydrogen accretors the range 59–65 min. There are no known accreting white dwarf binaries with an orbital period between 67 and 76 min. The periods were taken from Solheim (2010), Levitan et al. (2011), Ritter & Kolb (2003), Gänsicke et al. (2009), Augusteijn et al. (1996), Thorstensen et al. (2002), Littlefair et al. (2007) and Woudt et al. (2012). Individual periods are marked by ticks. The unclassified binaries CSS1028−0819 and CSS2333−1557 are included as CVs, but highlighted by a small horizontal bar. We use an abbreviated notation to indicate the periods of V485 Cen, EI Psc and CSS1122−1110.

the minimum period a system can reach is simply the level of hydrogen depletion when the mass transfer starts, there should be no reason not to find binaries in this period range (see e.g. Sienkiewicz 1984).

Unlike for EI Psc and V485 Cen, the secondary star is not detected in our spectra of CSS1122−1110 (see Fig. 1), which means that it must be of later spectral type than the K star seen in EI Psc. The argument for a very low mass, late-type donor (Section 3.4) is further supported by the mass ratios of those binaries, which are less extreme than that of CSS1122−1110. For V485 Cen, we use the $P_{\rm sh}$ measurement of Olech (1997) to calculate $q = 0.13 \pm 0.01$, and for EI Psc, the $P_{\rm sh}$ estimate from Uemura et al. (2002) gives $q = 0.14 \pm 0.01$. The mass ratio we find for CSS1122−1110 is much more extreme, $q = 0.017 \pm 0.004$. It is however similar to the mass ratios of the long-period AM CVn stars, e.g., GP Com ($P_{\rm orb} =$ 46.6 min, $q = 0.018$) and V396 Hya ($P_{\rm orb} = 65.1$ min, $q = 0.0125$) (both taken from Nelemans 2005), which suggests that it may be similarly evolved. Using a mass–radius relation for a fully degenerate helium star (private communication with Eggleton in Verbunt & Rappaport 1988), the mass of such a donor star at an orbital period of 65.233 min will be $0.006\,335\,{\rm M}_{\odot}$, which translates into $q_{\rm min} =$ 0.0076. This is even lower than the q measured for CSS1122−1110, indicating that the donor star in CSS1122−1110 is probably semidegenerate.

The observed properties of CSS1122−1110 strongly suggest that it is an AM CVn system forming via the evolved CV channel. All but the most extreme of AM CVn stars which evolve along the evolved CV channel are expected to have hydrogen left in the donor star. The system is expected to become increasingly helium rich as it evolves to shorter periods, but a small amount of hydrogen could still be left in the donor envelope as it passes the period minimum. The strong (compared to AM CVn stars) hydrogen lines in the spectrum of CSS1122−1110 may suggest that it is still evolving towards its minimum orbital period. The fact that it shows outbursts also supports this view, since the mass transfer rate must be high enough to trigger the disc thermal instability for outbursts to occur. This is in contrast with GP Com and V396 Hya which have never been observed in outburst, and are believed to have very low-mass transfer rates. AM CVns showing outbursts are generally found in the 20–40 min period range (e.g. Solheim 2010). On the other hand, the very low mass of the donor star could be interpreted as CSS1122−1110 having already evolved past its period minimum (Podsiadlowski et al. 2003, table A1).

A detailed abundance study may help to determine the evolutionary status of this binary. The relative abundances depend on a number of factors, such as the hydrogen abundance at the onset of mass transfer, the accretion rate and the temperature structure of the disc. Element abundances are difficult to measure, but Nagel, Rauch & Werner (2009) successfully reproduced the spectral features of V396 Hya using a non-local thermodynamic equilibrium accretion disc model. The line ratios we measure from the SDSS spectrum of CSS1122−1110 already suggest that the hydrogen content is very low compared to canonical CVs. We measure a flux ratio He I λ5876/Hα $= 1.49 \pm 0.04$, compared to He I λ5876/Hα $\sim 0.2-0.4$ for a typical dwarf novae (e.g. Szkody 1981; Thorstensen & Taylor 2001). A more detailed abundance analysis requires a high signal-to-noise spectrum covering a wide spectral range, but a suitable spectrum is not yet available for this system. The relative strengths of CNO species in such a spectrum will further help to distinguish between the different evolutionary scenarios (see Nelemans et al. 2010).

5 CONCLUSION

Time-resolved optical spectroscopy of the dwarf nova CSS1122−1110 reveals an orbital period of 65.233 ± 0.015 min, well below the CV period minimum. As is usual for CVs, the spectra are dominated by He I and Balmer emission lines, but the He I lines are unusually strong, likely a sign of high helium abundance. The Hα and He I λ 6678 lines display a narrow emission component, stationary at the line centre to within 16 km s^{-1}. Using Doppler maps, we can associate this 'central spike' with emission from the white dwarf. Such a triple-peaked emission line structure, with a central spike originating from near the white dwarf, is a characteristic only seen in helium-dominated systems, not in CVs. We combine our spectroscopically measured orbital period with the superhump period measured by Kato et al. (2010) to find an extreme mass ratio for this binary, $q = 0.017 \pm 0.004$. Using the average CV white dwarf mass, this implies a very low-mass donor star, $M_2 =$ $(0.014 \pm 0.005)\,{\rm M}_{\odot}$. Comparing the properties of this ultracompact accreting binary with CVs, AM CVn systems and hydrogen binaries below the CV period minimum, we argue that CSS1122−1110 is the first compelling example of an AM CVn system forming via the evolved CV channel.

ACKNOWLEDGMENTS

We thank our referee, M. Wood, for his suggestions and comments on this paper. EB, BTG, TRM, DS and CMC acknowledge support from the UK STFC in the form of a Rolling Grant. This paper is based on observations made with the ESO's VLT, as part of programme 086.D-0243B. The CSS survey is funded by the National Aeronautics and Space Administration under Grant No. NNG05GF22G issued through the Science Mission Directorate Near-Earth Objects Observations Programme. The CRTS survey

is supported by the U.S. National Science Foundation under grant AST-0909182.

REFERENCES

Abazajian K. N. et al., 2009, ApJS, 182, 543
Aihara H. et al., 2011, ApJS, 193, 29
Augusteijn T., van Kerkwijk M. H., van Paradijs J., 1993, A&A, 267, L55
Augusteijn T., van der Hooft F., de Jong J. A., van Paradijs J., 1996, A&A, 311, 889
Brown W. R., Kilic M., Hermes J. J., Allende Prieto C., Kenyon S. J., Winget D. E., 2011, ApJ, 737, L23
Brown W. R., Kilic M., Allende Prieto C., Kenyon S. J., 2012, ApJ, 744, 142
Copperwheat C. M. et al., 2011, MNRAS, 410, 1113
Drake A. J. et al., 2009, ApJ, 696, 870
Faulkner J., Flannery B. P., Warner B., 1972, ApJ, 175, L79
Gänsicke B. T., 2005, in Hameury J.-M., Lasota J.-P., eds, ASP Conf. Ser. Vol. 330, The Astrophysics of Cataclysmic Variables and Related Objects. Astron. Soc. Pac., San Francisco, p. 3
Gänsicke B. T. et al., 2003, ApJ, 594, 443
Gänsicke B. T., Araujo-Betancor S., Hagen H.-J., Harlaftis E. T., Kitsionas S., Dreizler S., Engels D., 2004, A&A, 418, 265
Gänsicke B. T. et al., 2009, MNRAS, 397, 2170
Hirose M., Osaki Y., 1990, PASJ, 42, 135
Iben I., Jr, Tutukov A. V., 1987, ApJ, 313, 727
Kato T., 2010, vsnet-alert, 12026
Kato T., Kinugasa K., 2009, vsnet-alert, 11166
Kato T. et al., 2009, PASJ, 61, 395
Kato T. et al., 2010, PASJ, 62, 1525
Knigge C., 2006, MNRAS, 373, 484
Kolb U., Baraffe I., 1999, MNRAS, 309, 1034
Levitan D. et al., 2011, ApJ, 739, 68
Littlefair S. P., Dhillon V. S., Marsh T. R., Gänsicke B. T., Baraffe I., Watson C. A., 2007, MNRAS, 381, 827
Lomb N. R., 1976, Ap&SS, 39, 447
Maehara H., 2010a, vsnet-alert, 12020
Maehara H., 2010b, vsnet-alert, 12025
Marsh T. R., 1989, PASP, 101, 1032
Marsh T. R., 1999, MNRAS, 304, 443
Marsh T. R., Horne K., 1988, MNRAS, 235, 269
Martin D. C. et al., 2005, ApJ, 619, L1
Morales-Rueda L., Marsh T. R., Steeghs D., Unda Sanzana E., Wood J. H., North R. C., 2003, A&A, 405, 249
Nagel T., Rauch T., Werner K., 2009, A&A, 499, 773
Nelemans G., 2005, in Hameury J.-M., Lasota J.-P., eds, The Astrophysics of Cataclysmic Variables and Related Objects. Astron. Soc. Pac., San Francisco, p. 27
Nelemans G., Yungelson L. R., Portegies Zwart S. F., 2004, MNRAS, 349, 181
Nelemans G., Yungelson L. R., van der Sluys M. V., Tout C. A., 2010, MNRAS, 401, 1347
Olech A., 1997, Acta Astron., 47, 281
Osaki Y., 1989, PASJ, 41, 1005
Paczyński B., 1967, Acta Astron., 17, 287
Patterson J. et al., 2005, PASP, 117, 1204
Podsiadlowski P., Han Z., Rappaport S., 2003, MNRAS, 340, 1214
Pylyser E. H. P., Savonije G. J., 1989, A&A, 208, 52
Rappaport S., Joss P. C., Webbink R. F., 1982, ApJ, 254, 616
Ritter H., Kolb U., 2003, A&A, 404, 301
Roelofs G. H. A., Groot P. J., Marsh T. R., Steeghs D., Barros S. C. C., Nelemans G., 2005, MNRAS, 361, 487
Roelofs G. H. A., Rau A., Marsh T. R., Steeghs D., Groot P. J., Nelemans G., 2010, ApJ, 711, L138
Ruiz M. T., Rojo P. M., Garay G., Maza J., 2001, ApJ, 552, 679
Savonije G. J., de Kool M., van den Heuvel E. P. J., 1986, A&A, 155, 51
Scargle J. D., 1982, ApJ, 263, 835
Schenker K., King A. R., Kolb U., Wynn G. A., Zhang Z., 2002, MNRAS, 337, 1105
Schlegel D. J., Finkbeiner D. P., Davis M., 1998, ApJ, 500, 525
Schneider D. P., Young P., 1980, ApJ, 240, 871
Shafter A. W., 1983, ApJ, 267, 222
Shafter A. W., Szkody P., Thorstensen J. R., 1986, ApJ, 308, 765
Sienkiewicz R., 1984, Acta Astron., 34, 325
Smak J., 1975, Acta Astron., 25, 227
Solheim J.-E., 2010, PASP, 122, 1133
Southworth J., Marsh T. R., Gänsicke B. T., Steeghs D., Copperwheat C. M., 2010, A&A, 524, A86
Steeghs D., Horne K., Marsh T. R., Donati J. F., 1996, MNRAS, 281, 626
Szkody P., 1981, ApJ, 247, 577
Szkody P. et al., 2011, AJ, 142, 181
Tappert C., Gänsicke B. T., Rebassa-Mansergas A., Schmidtobreick L., Schreiber M. R., 2011a, A&A, 531, A113
Tappert C., Gänsicke B. T., Schmidtobreick L., Ribeiro T., 2011b, A&A, 532, A129
Thorstensen J. R., 2000, PASP, 112, 1269
Thorstensen J. R., Taylor C. J., 2001, MNRAS, 326, 1235
Thorstensen J. R., Fenton W. H., Patterson J. O., Kemp J., Krajci T., Baraffe I., 2002, ApJ, 567, L49
Tutukov A. V., Fedorova A. V., Ergma E. V., Yungelson L. R., 1985, Soviet Astron. Lett., 11, 52
Uemura M. et al., 2002, PASJ, 54, 599
Uthas H., Knigge C., Long K. S., Patterson J., Thorstensen J., 2011, MNRAS, 414, L85
van der Sluys M. V., Verbunt F., Pols O. R., 2005a, A&A, 431, 647
van der Sluys M. V., Verbunt F., Pols O. R., 2005b, A&A, 440, 973
Verbunt F., Rappaport S., 1988, ApJ, 332, 193
Warner B., 1995, Cataclysmic Variable Stars. Cambridge Univ. Press, Cambridge
Whitehurst R., 1988, MNRAS, 232, 35
Wood M. A., Still M. D., Howell S. B., Cannizzo J. K., Smale A. P., 2011, ApJ, 741, 105
Woudt P. A., Warner B., 2011, Astron. Telegram, 3705, 1
Woudt P. A., Warner B., de Budé D., Macfarlane S., Schurch M. P. E., Zietsman E., 2012, MNRAS, 421, 2414
Zorotovic M., Schreiber M. R., Gänsicke B. T., 2011, A&A, 536, A42

This paper has been typeset from a TEX/LATEX file prepared by the author.